Beamwidth Optimization for 5G NR Millimeter Wave Cellular Networks: A Multi-armed Bandit Approach

Mingjie Feng[1], Berk Akgun[2], Irmak Aykin[2], and Marwan Krunz[1]
[1]Dept. Electrical & Computer Engineering, The University of Arizona, Tucson, AZ 58721 USA
[2]Qualcomm Inc., San Diego, CA 92121 USA
Email: mingjiefeng@email.arizona, berkakgun@email.arizona.edu, aykin@email.arizona.edu, krunz@email.arizona.edu

***Abstract*—The use of highly directional antennas in millimeter wave (mmWave) cellular networks necessitates precise beam alignment between a base station (BS) and a user equipment (UE), which requires beam sweeping over a large number of directions and causes high initial access (IA) delay. Intuitively, such delay can be lowered by using wider beams, as fewer directions need to be swept. However, this results in a weak received signal and higher misdetection probability, which in turn increases the IA delay as more rounds of beam sweeping would be required to discover a UE. In this paper, we propose a multi-armed bandit approach for beamwidth optimization in 5G New Radio (NR) mmWave cellular networks. We aim to find the optimal beamwidths at the BS and the UE that minimize the beam sweeping delay for a successful IA. We first formulate the beamwidth optimization problem based on analyzing the interplay among beamwidth, beam sweeping overhead, and misdetection probability. Then, we propose a two-stage solution framework based on a multi-armed bandit approach. In the first stage, an initial solution of the BS beamwidth and the optimal solution of UE beamwidth are derived. In the second stage, each BS learns its optimal beamwidth by solving a multi-armed bandit problem with a Thompson sampling-based algorithm. Our extensive simulation results show that, the proposed algorithms can decrease the IA delay by more than 50% compared to the traditional fixed-beamwidth schemes.**

***Index Terms*—Millimeter wave cellular network; 5G NR; initial access; beamwidth optimization; multi-armed bandit.**

I. Introduction

Millimeter wave (mmWave) communications is one of the enabling technologies for Fifth Generation (5G) wireless systems [1]. By operating at mmWave bands, multi-Gbps data rates per user can be achieved. Due to their great potential, mmWave bands are utilized by both next generation WLANs (e.g., 802.11ad and 802.11ay) as well as 5G New Radio (NR).

At the same time, mmWave communications suffer from large propagation losses, limited scattering, and vulnerability to blockage. To compensate for channel losses, large electronically steerable antenna arrays can be employed at both the transmitter (Tx) and the receiver (Rx) to achieve highly directional transmissions/receptions with high antenna gains. However, the use of narrow beams complicates the initial access (IA) in mmWave cellular networks. IA is the process for network discovery and establishing a connection between a user equipment (UE) and a base station (BS). Typically, IA requires beam alignment to find the best BS-UE beam pair through a beam sweeping process. In 5G NR systems, beam sweeping is performed using a series of synchronization signals (SS) that are transmitted and received along different directions. As narrow beams are used, a large number of directions need to be sequentially scanned to cover the entire angular domain, resulting in high IA delay.

An intuitive approach to lower the IA delay is using wider beams to decrease the number of directions used during beam sweeping. Such an approach, which has been adopted in both WLANs [2] and cellular networks [3], is based on a two-stage hierarchical search. In the first stage, a small number of wide sectors (or cones in 3D search) are swept (known as P1 in 5G NR). In the second stage, the search is refined within the best-found coarse sector (known as P2 at the BS side and P3 at the UE side in 5G NR). However, with wider beams, the received power decreases significantly due to lower antenna gains. In addition, when signals are transmitted and received over wide sectors, it is more likely that several signal clusters will be received within the same sector. Due to the phase difference, these clusters may add destructively, which potentially degrades the received signal. If no SS is detected during one round of beam sweeping, additional rounds will be required, resulting in increased IA delay.

Considering the tradeoff between the increased likelihood of misdetection under wider beams and the higher beam sweeping overhead under narrower beams, the optimal beamwidths at the BS and the UE need to be optimized to minimize the beam sweeping delay for a successful IA. From the perspective of a UE, the misdetection probability is low when the channel between the UE and the BS is strong, which allows the UE to use wide beams to reduce the beam sweeping overhead. Conversely, when the channel between the BS and the UE is weak, narrow beams should be used to improve the success rate of SS detection. For a BS, its beamwidth selection during IA impacts the delays of all UEs that are trying to connect to the BS. Thus, the beamwidth at the BS needs to be adjusted based on the channel statistics of all UEs.

In this paper, we consider beamwidth optimization for standalone (SA) 5G NR mmWave cellular networks and propose a two-stage solution framework based on a multi-armed bandit (MAB) approach. In the first stage, the initial solution of beamwidth optimization is derived by based on the channel

statistics and the distribution of BS-UE distance. In the second stage, an online beamwidth adaptation scheme is developed, where each BS to learn its optimal beamwidth from the measured beam sweeping delays. Such a scheme only requires a BS to perform a simple calculation for parameter update at each iteration of learning, making it easy to implement. The contributions of this paper are as follows:

- We formulate the beamwidth optimization problem with the objective of minimizing the average beam sweeping delay, considering the effect of misdetection.
- We analyze the impact of beamwidth on UE detection and derive the misdetection probability.
- We propose a two-stage framework for finding the optimal beamwidths at the BS and the UE during beam sweeping. The first stage provides an initial solution of the BS beamwidth and the optimal solution of UE beamwidth. In the second stage, the BS beamwidth selection is formulated as an MAB problem, which is solved by a Thompson sampling (TS)-based algorithm.
- We evaluate the performance of the proposed algorithms via simulations. Our results show that, on average, the proposed algorithms lower the beam sweeping delay by 50% compared to the classical fixed beamwidth scheme.

In the remainder of this paper, we first review related literature in Section II. Then, we present the system model in Section III, followed by the misdetection analysis and problem formulation in Section IV and V, respectively. Next, the solution algorithms are introduced in Section VI. We then depict the simulation results and conclude the paper in Section VII and VIII, respectively.

II. Related Work

IA protocols for mmWave cellular systems have been extensively studied, where a few analytical frameworks were presented in [14], [15]. The IA specified by 3GPP for mmWave cellular networks was summarized in [7]. To reduce the IA delay, the sparsity of mmWave channels was utilized to reduce the search overhead [16], [17]. The search overhead can also be reduced with random beamforming, where instead of search all directions, a random subset of directions are selected for beam sweeping [4], [18]. In this paper, we minimize the beam sweeping delay via beamwidth optimization. Our approach can be combined with many approaches mentioned above.

Beamwidth optimization for mmWave systems was considered in existing works, e.g., in [2], [4], [5]. However, the interplay among the beamwidth, the misdetection probability, and the beam sweeping overhead under the context of 5G NR has not been analyzed in these works. Besides, the analysis is based on a single-path LOS channel model, which does not capture the effect of receiving signals from multiple clusters. In contrast, we analyze the impact of beamwidth on the misdetection probability and the expected beam sweeping delay to enable beamwidth optimization, and our analysis is based on a multipath propagation environment. Most importantly, our scheme is based on a low-complexity online learning process, which is easy to implement.

Misdetection aware beamwidth optimization was investigated recently (e.g., in [5], [18]). In these works, beamwidth optimization was only applied to the BS, hence the benefit of adjusting UE beamwidth for delay reduction has not been harnessed. Besides, the analytical frameworks in these works are not based on 5G NR, thus the solution cannot be applied to our problem. In contrast, our solution is specifically designed for the 5G NR standard and we optimize the beamwidths at both the BS and the UE.

III. System Model

A. Network Model

We consider a cellular mmWave system that consists of multiple BSs and UEs, whose locations are randomly distributed according to Poisson Point Processes (PPP) of densities ρ_{BS} and ρ_{UE}, respectively. Let r be the distance between an arbitrary UE and its serving BS (for simplicity, we assume that each UE is served by the nearest BS). Then, the probability density function (PDF) of r is given by [6]:

$$f_r(r) = 2\pi\rho_{\mathrm{BS}} r e^{-\rho_{\mathrm{BS}}\pi r^2}, r > 0. \tag{1}$$

B. Antenna Model and Beamwidth Adaptation

We assume that the BSs and UEs are equipped with uniform linear arrays (ULAs) with M_{BS} and M_{UE} active antenna elements, respectively. The beamwidth at BS and UE can be changed by adjusting M_{BS} and M_{UE}, respectively. Specifically, when the beam is directed towards the broadside of the antenna array, the half-power beamwidth (HPBW) of the resulting far-field antenna pattern can be estimated as [11]:

$$\theta_{\mathrm{BS}} \approx \frac{0.886\lambda}{d \cdot M_{\mathrm{BS}}},\ \theta_{\mathrm{UE}} \approx \frac{0.886\lambda}{d \cdot M_{\mathrm{UE}}}, \tag{2}$$

where λ is the wavelength and d is the antenna spacing. For analytical tractability, we approximate the actual antenna patterns by a sectored antenna model, as often done in the literature [20]. Let $G_{\mathrm{BS}}(\eta')$ and $G_{\mathrm{UE}}(\eta)$ be the antenna gain of the BS and the antenna gain of the UE when the angles off the broadside are η' and η, respectively, where $\eta, \eta' \in [0, 2\pi]$. $G_{\mathrm{BS}}(\eta')$ and $G_{\mathrm{UE}}(\eta)$ can be written as:

$$G_{\mathrm{BS}}(\eta') = \begin{cases} M_{\mathrm{BS}}, & \text{if } |\eta'| \le \frac{\theta_{\mathrm{BS}}}{2} \\ 0, & \text{otherwise,} \end{cases}$$
$$G_{\mathrm{UE}}(\eta) = \begin{cases} M_{\mathrm{UE}}, & \text{if } |\eta| \le \frac{\theta_{\mathrm{UE}}}{2} \\ 0, & \text{otherwise.} \end{cases} \tag{3}$$

Let $\theta_{\mathrm{BS}}^{(1)}$ and $\theta_{\mathrm{BS}}^{(2)}$ be the BS beamwidths used in P1 (coarse beam sweeping) and P2 (refined beam sweeping) respectively; $\theta_{\mathrm{UE}}^{(1)}$ and $\theta_{\mathrm{UE}}^{(2)}$ be the UE beamwidths used in P1 (coarse) and P3 (refined) respectively. The minimum required number of beam directions to cover the entire 2-dimension angular space at the BS and the UE during P1–P3 are given by:

$$N_{\mathrm{BS}}^{(1)} = \left\lceil \frac{2\pi}{\theta_{\mathrm{BS}}^{(1)}} \right\rceil,\ N_{\mathrm{UE}}^{(1)} = \left\lceil \frac{2\pi}{\theta_{\mathrm{UE}}^{(1)}} \right\rceil,$$
$$N_{\mathrm{BS}}^{(2)} = \left\lceil \frac{2\pi}{\theta_{\mathrm{BS}}^{(1)}\theta_{\mathrm{BS}}^{(2)}} \right\rceil,\ N_{\mathrm{UE}}^{(2)} = \left\lceil \frac{2\pi}{\theta_{\mathrm{UE}}^{(1)}\theta_{\mathrm{UE}}^{(2)}} \right\rceil. \tag{4}$$

C. SS Blocks for Beam Sweeping

In 5G NR, SS blocks are used for beam sweeping. An SS block consists of 4 consecutive OFDM symbols in the time domain and 240 subcarriers in the frequency domain [8]. These SS blocks carry the Primary Synchronization Signal (PSS), the Secondary Synchronization Signal (SSS), and Physical Broadcast Channel (PBCH). In particular, the Demodulation Reference Signal (DMRS) in the PBCH is used to estimate the reference signal received power (RSRP) of the SS block.

During beam sweeping, the BS periodically sends SS blocks along different directions. The serving beam index information is also contained in the PBCH, which is used by the UE when reporting the best beam back to the BS. SS blocks are sent within an SS burst, whose duration is 5 ms and periodicity is $T_{\rm SS}$, where $T_{\rm SS} \in \{5, 10, 20, 40, 80, 160\}$ ms.

D. Communication Model

We use the statistical channel model from NYU Poly [12]. The channel between the BS and the UE is composed by a set of distinctive clusters, each corresponds to a scattering path. The AoD/AoA of each cluster at the BS/UE is uniformly distributed in $(0, 2\pi)$. During beam sweeping, if the AoD/AoA of a cluster is not in the range of a BS/UE sector, the cluster cannot be utilized to transmit/receive SS blocks.

Let C be the number of clusters. Due to the directional Tx/Rx, only a subset of the C clusters would be utilized by each BS sector for SS block transmission. Let L be the number of clusters utilized by a BS sector, $L \leq C$. Similarly, each UE sector would only utilize a subset of the L clusters to receive SS blocks. Let K be the number of clusters utilized by a UE sector, $K \leq L$. The value of L determines the distribution of power fraction for each cluster, and the value of K determines Rx power gain under when multiple clusters are combined. Thus, the power gain between the BS and the UE is a function of both L and K. The received power of an SS block at UE under given L and K is given by:

$$P_{\rm UE} = P_{\rm BS} \cdot G_{\rm BS} \cdot G_{\rm UE} \cdot {\rm PL}^{-1} \cdot \gamma_{\rm L,K} \tag{5}$$

where $P_{\rm BS}$ is the BS transmission power, PL is the distance-dependent path loss between BS and UE, $\gamma_{L,K}$ is the power scaling factor when L clusters are transmitted from a BS sector and K of them are received by the UE in the same sector. Using the model from [12], the distribution of $\gamma_{L,K}$ can be numerically derived.

IV. Misdetection Probability Analysis

We define misdetection as the incident where no SS block is successfully received by the UE during a complete round of beam sweeping. The UE fails to receive an SS block when the received power is below a threshold $P_{\rm th}$. We first consider the reception of SS blocks at a fixed UE sector. Let $\mathcal{P}_{L,K}^{\rm Sec}$ be the probability that a UE fails to detect any SS block in that sector with given L and K. Follow (5), $\mathcal{P}_{L,K}^{\rm Sec}$ is given by:

$$\mathcal{P}_{L,K}^{\rm Sec} = \Pr\left\{\gamma_{L,K} \leq \frac{P_{\rm th} \cdot {\rm PL}}{P_{\rm BS} \cdot G_{\rm BS} \cdot G_{\rm UE}}\right\}. \tag{6}$$

Using the numerically derived PDF of $\gamma_{L,K}$ and empirical path loss model (e.g.,from [12]), $\mathcal{P}_{L,K}^{\rm Sec}$ can be calculated.

As beam sweeping proceeds, the values of L and K for each pair of BS sector and UE sector varies, resulting in different misdetection probability for each pair. To calculate the misdetection probability of a complete round of beam sweeping, it is necessary to integrate the misdetection probabilities of all pairs. The values of L and K for all pairs of BS sector and UE sector are determined by how the clusters are distributed among different BS and UE sectors. As the AoAs/AoDs of all clusters are randomly distributed, there are various such distributions, each with a certain probability. We index the possible distributions of clusters at BS and UE by $u = 1, 2, \ldots, U$ and $v = 1, 2, \ldots, V$, respectively. Then, we define two sets of binary variables, δ_u and π_v, as indicators of these distributions. Specifically, $\delta_u = 1$ indicates that the u th BS cluster distribution occurs and $\delta_u = 0$ indicates otherwise; $\pi_v = 1$ indicates that the v th UE cluster distribution occurs and $\pi_v = 0$ indicates otherwise. We denote the u th distribution by the vector $[L_u^C(1), L_u^C(2), ..., L_u^C(N_{\rm BS})]$. Then, $\sum_{i=1}^{N_{\rm BS}} L_u^C(i) = C$ holds for $u = 1, ..., U$. The v th distribution is given by the vector $K_v^L(1), K_v^L(2), ..., K_v^L(N_{\rm UE})$, then we have $\sum_{j=1}^{N_{\rm UE}} K_v^L(j) = L, v = 1, ..., V$.

With C clusters distributed in $N_{\rm BS}$ sectors at the BS, the total number of possible distributions is $N_{\rm BS}^C$. Depending on $N_{\rm BS} \geq C$ or $N_{\rm BS} < C$, the probability of each distribution is calculated in different ways based on probability theory. Due to page limit, we omit the detailed calculations.

Next, we consider the misdetection probability when SS blocks are sent via a fixed BS sector and are received by *all* UE sectors. This probability is calculated by multiplying the misdetection probabilities of all UE sectors. With multiple possible cluster distributions at the UE ($v = 1, ..., V$), the average misdetection probability is a weighted sum of misdetection probabilities under all possible distributions, given by:

$$\mathcal{P}_L^{\rm UE} = \sum_{v=1}^{V} \left\{ \Pr\{\pi_v = 1\} \cdot \prod_{j=1}^{N_{\rm UE}} \mathcal{P}_{L,K_v^L(j)}^{\rm Sec} \right\}. \tag{7}$$

Note that no SS block will be received for the UE sectors with no path/cluster in their ranges. Thus, the misdetection probability for these sectors is 1, which do not impact the product given in (7). This also applies to the BS sectors. As a result, we only need to consider the sectors with paths/clusters in their ranges in our calculation.

We then consider the scenario that SS blocks are sequentially sent from *all* BS sectors, which is a complete round of beam sweeping for all $N_{\rm BS}N_{\rm UE}$ sectors. The misdetection probability under this scenario is the product of misdetection probabilities when the SS blocks are sent from all BS sectors. With different cluster distributions at the BS ($u = 1, ..., U$), and for a given C, the average misdetection probability is a weighted sum of misdetection probabilities under different

cluster distributions at BS, given by:

$$\mathcal{P}_{\text{mis}}^{C} = \sum_{u=1}^{U} \left\{ \Pr\{\delta_u = 1\} \cdot \prod_{i=1}^{N_{\text{BS}}} \mathcal{P}_{L_u^C(i)}^{\text{UE}} \right\}. \tag{8}$$

Based on [12], C is a random variable given by $C \sim \max\{\text{Poisson}(\kappa), 1\}$, where $\kappa = 1.8$ at 28 GHz and $\kappa = 1.9$ at 73 GHz.

Finally, the average misdectection probability for a complete round of beam sweeping is:

$$\mathcal{P}_{\text{mis}} = \sum_{C'=1}^{\infty} \left\{ \Pr\{C = C'\} \cdot \mathcal{P}_{\text{mis}}^{C'} \right\}. \tag{9}$$

V. Problem Formulation

In the NR framework, the number of SS blocks required to complete one round of beam sweeping is determined by the total number of beam pairs, given by $N_{\text{BS}}^{(1)} N_{\text{UE}}^{(1)}$ for the first stage (coarse, P1 of BS and UE) and $N_{\text{BS}}^{(2)} N_{\text{UE}}^{(2)}$ for the second stage (refined, P2 of BS and P3 of UE), respectively[1]. Let $\mathcal{P}_{\text{mis}}^{(1)}$ and $\mathcal{P}_{\text{mis}}^{(2)}$ denote the misdetection probability for one round of beam sweeping during the first and second stage, respectively. When misdetection occurs, the UE needs to wait for the next round of beam sweeping, until the successful reception of an SS block. Then, the probability that n rounds of first stage beam sweeping is required follows a geometric distribution, given by $(1 - \mathcal{P}_{\text{mis}}^{(1)}){\mathcal{P}_{\text{mis}}^{(1)}}^{n-1}$. The same result applies to the second stage of beam sweeping. Let n and m be the numbers of rounds required for the first and second stage of beam sweeping, respectively. The total number of beam sweep directions is given by:

$$N_{\text{tot}} = n N_{\text{BS}}^{(1)} N_{\text{UE}}^{(1)} + m N_{\text{BS}}^{(2)} N_{\text{UE}}^{(2)}. \tag{10}$$

Let N_{SS} be the number of SS blocks in each SS burst. Then, the number of SS bursts needed is $\left\lfloor \frac{N_{\text{tot}}}{N_{\text{SS}}} \right\rfloor$. In the last SS burst, the number of utilized SS blocks is $N_{\text{last}} = N_{\text{tot}} - N_{\text{SS}} \left\lfloor \frac{N_{\text{tot}}}{N_{\text{SS}}} \right\rfloor$. In 5G NR, two SS blocks are transmitted in each slot, and therefore, the number of slots needed in the last SS burst is $\frac{N_{\text{last}}}{2}$. Given the period of SS bursts T_{SS} and the duration of a time slot T_{slot}, the expected beam sweeping delay of a UE can be written as:

$$\overline{D} = \sum_{n=1}^{\infty} (1 - \mathcal{P}_{\text{mis}}^{(1)}) {\mathcal{P}_{\text{mis}}^{(1)}}^{n-1} (1 - \mathcal{P}_{\text{mis}}^{(2)}) {\mathcal{P}_{\text{mis}}^{(1)}}^{m-1} \left[T_{\text{SS}} \left\lfloor \frac{N_{\text{tot}}}{N_{\text{SS}}} \right\rfloor + \frac{T_{\text{slot}}}{2} \left(N_{\text{tot}} - N_{\text{SS}} \left\lfloor \frac{N_{\text{tot}}}{N_{\text{SS}}} \right\rfloor \right) \right]. \tag{11}$$

Given the distribution of r, the expected delay of all UEs in the coverage of a BS is given by:

$$\mathbb{E}[D] = \int_0^{\infty} \overline{D}(r) f_r(r) \mathrm{d}r \tag{12}$$

[1]For power efficiency, we assume an analog beamforming architecture in which the BS and/or the UE cannot scan multiple directions simultaneously.

where $f_r(r)$ is the PDF of r given in (1). Then, the expected delay minimization problem can be written as:

$$\min_{\left\{N_{\text{BS}}^{(1)}, N_{\text{BS}}^{(2)}, N_{\text{UE}}^{(1)}, N_{\text{UE}}^{(2)}\right\}} \mathbb{E}[D]$$
$$\text{subject to: } N_{\text{BS}}^{(1)}, N_{\text{BS}}^{(2)} \in \Omega_{\text{BS}},$$
$$N_{\text{UE}}^{(1)}, N_{\text{UE}}^{(2)} \in \Omega_{\text{UE}}.$$

Where Ω_{BS} and Ω_{UE} are the sets of feasible values of BS beamwidth and UE beamwidth, respectively. The elements in Ω_{BS} and Ω_{UE} are determined by the possible antenna configurations at the BS and the UE as explained in Section III. Obviously, $\mathcal{P}_{\text{mis}}^{(1)}$ and $\mathcal{P}_{\text{mis}}^{(2)}$ are the functions of $(N_{\text{BS}}^{(1)}, N_{\text{UE}}^{(1)}, r)$ and $(N_{\text{BS}}^{(2)}, N_{\text{UE}}^{(2)}, r)$, respectively.

VI. Solution Algorithms

In this section, we present the MAB-based solution algorithms. For notational simplicity, we denote $\mathbf{N}_{\text{BS}} \triangleq [N_{\text{BS}}^{(1)}, N_{\text{BS}}^{(2)}]$ and $\mathbf{N}_{\text{UE}} \triangleq [N_{\text{UE}}^{(1)}, N_{\text{UE}}^{(2)}]$. The solution algorithms have two stages. At the first stage, the optimal $[\mathbf{N}_{\text{BS}}, \mathbf{N}_{\text{UE}}]$ that minimize $\mathbb{E}[D]$, denoted by $[\mathbf{N}_{\text{BS}}^*, \mathbf{N}_{\text{UE}}^*]$, are obtained based on the BS density ρ_{BS}. In the second stage, each BS further adapts $\mathbf{N}_{\text{BS}}$ by solving a MAB problem.

A. First Stage

A UE in an SA system has no information about the BS that it will be connecting to until the IA is completed. Thus, N_{UE} should be set to a default value that is known by all BSs owned by the same operator. As a UE may roam in areas with varying BS densities, we set $\mathbf{N}_{\text{UE}}$ to the optimal value when $\rho_{\text{BS}} = \overline{\rho}_{\text{BS}}$. Then, $\mathbf{N}_{\text{UE}}^*$ is obtained by:

$$\left[\mathbf{N}_{\text{BS}}^*, \mathbf{N}_{\text{UE}}^*\right] = \arg \min_{\{\mathbf{N}_{\text{BS}}, \mathbf{N}_{\text{UE}}\}} \mathbb{E}[D] \tag{13}$$

where $\mathbb{E}[D]$ is calculated by (12) with $\rho_{\text{BS}} = \overline{\rho}_{\text{BS}}$. The search in (13) is performed offline by the operator.

The beamwidth at each BS is optimized by:

$$\mathbf{N}_{\text{BS}}^* = \arg \min_{\mathbf{N}_{\text{BS}}} \mathbb{E}[D]. \tag{14}$$

In (14), $\mathbb{E}[D]$ is calculated by (12) with ρ_{BS} and N_{UE}^*. The optimization of (14) is performed offline by each BS.

B. Second Stage

Based on the outcome of the first stage, each BS further adapts its beamwidth. Specifically, each BS acts as an agent who plays one arm at each time step ($t = 1, \ldots, T$) and learns to find the arm with minimum average penalty. The arms to be played are the possible selections of BS beamwidths, denoted by $\mathbf{N}_{\text{BS}}^i$, $i = 1, \ldots, \Phi_{\text{BS}}$, where Φ_{BS} is the number of possible $\mathbf{N}_{\text{BS}}^i$. Let d_i be the mean penalty for playing arm i, it is defined as the *normalized* average delay when the BS beamwidth is set to be $\mathbf{N}_{\text{BS}}^i$:

$$d_i = \min\left(\frac{\overline{D}(\mathbf{N}_{\text{BS}}^i)}{D_{\text{ref}}}, 1 \right) \tag{15}$$

where $\overline{D}(\mathbf{N}_{\mathrm{BS}}^i)$ is the average delay of all UEs when $\mathbf{N}_{\mathrm{BS}} = \mathbf{N}_{\mathrm{BS}}^i$, D_{ref} is a sufficiently large reference delay. The normalization given by (15) is necessary for applying the TS algorithm given in [21]. The main objective of TS-based learning is to find the arm with the minimum d_i.

The average delay of all UEs used for learning is measured by the BS over a relatively long period of time (e.g., multiple rounds of SS bursts). This way, the beamwidth selection is performed in a larger time scale than that of beam sweeping and the effect of channel variation is averaged out. To obtain the average delay, each UE has a timer that records its beam sweeping delay and reports it to the BS when IA is completed. At the end of each time step, the BS use all reported delays to calculate the average delay during that period.

At each step of the TS-based learning, the BS keeps a belief about the distribution of d_i, $i = 1, \ldots, \Phi_{\mathrm{BS}}$, and samples all arms according to such belief. Then, it plays the arm with the minimum sampled value and observes the penalty for playing that arm. After that, it updates the belief of the played arm based on the observed penalty. Such an update can be implemented with Bayesian inference, which calculates the posterior distribution based on the observed data and prior distribution. Based on the TS algorithm described in [21] and given that $0 \leq d_i \leq 1$, Beta distribution is the conjugate prior of the distribution of d_i. This is because the posterior of a Beta distribution is also a Beta distribution, which makes the parameter update at each round of the TS algorithm easy to implement. Let $\hat{d}_i^{[t]}$ be the prior distribution of d_i at time t, we have $\hat{d}_i^{[t]} \sim \mathrm{Beta}(\alpha_i^{[t]}, \beta_i^{[t]})$, $i = 1, \ldots, \Phi_{\mathrm{BS}}$, where $\alpha_i^{[t]}$ and $\beta_i^{[t]}$ are the parameters of the Beta distribution. The PDF of a Beta distribution is given by $f(x; \alpha, \beta) = \frac{\Gamma(\alpha+\beta)}{\Gamma(\alpha)\Gamma(\beta)} x^{\alpha-1}(1-x)^{\beta-1}$, with mean $\frac{\alpha}{\alpha+\beta}$.

To accelerate the convergence of the TS algorithm, we use the outcome of the first stage to generate the initial distribution of each d_i. Without such initialization, the BS may spend a significant amount of time on the arms with a large delay. To obtain the initial distribution of d_i, we first calculate $\mathbb{E}[D(\mathbf{N}_{\mathrm{BS}}^i)]$ by (12) based on $\mathbf{N}_{\mathrm{BS}}^i$, ρ_{BS}, and $\mathbf{N}_{\mathrm{UE}}^*$. Then, we find a set of $(\alpha_i^{[1]}, \beta_i^{[1]})$ to approximate the normalized $\mathbb{E}[D(\mathbf{N}_{\mathrm{BS}}^i)]$ as follow:

$$\frac{\alpha_i^{[1]}}{\alpha_i^{[1]} + \beta_i^{[1]}} \approx \min\left(\frac{\mathbb{E}[D(\mathbf{N}_{\mathrm{BS}}^i)]}{D_{\mathrm{ref}}}, 1\right). \tag{16}$$

For example, suppose $\frac{\mathbb{E}[D(\mathbf{N}_{\mathrm{BS}}^i)]}{D_{\mathrm{ref}}} = 0.78$ (suppose keep two numbers after decimal), we can set $\alpha_i^{[1]} = 78, \beta_i^{[1]} = 22$.

With the initial distributions of d_i, each BS performs the TS algorithm given in Algorithm 1. At each time t, the BS samples the arms $i = 1, \ldots, \Phi_{\mathrm{BS}}$ according their PDFs, plays the arm with minimum sampled value, observes the penalty, and updates the parameters of the selected arm. The observed penalty is the *normalized* average beam sweeping delay of all UEs, calculated by:

$$\Theta^{[t]} = \min\left(\frac{\overline{D}(\mathbf{N}_{\mathrm{BS}}^{i^*})}{D_{\mathrm{ref}}}, 1\right). \tag{17}$$

Algorithm 1: TS-based BS Beamwidth Adaptation

```
Initialize: Set (α_i^[1], β_i^[1]) (i = 1, ..., Φ_BS) according to (16);
d̂_i^[1] ~ Beta(α_i^[1], β_i^[1]), i = 1, ..., |Ω_BS|;
for t = 1 : T do
    for i = 1 : |Ω_BS| do
        Sample d̂_i^[t] from Beta(α_i^[t], β_i^[t]) with outcome e_i^[t];
    end
    Play arm i* = arg min_i e_i^[t] and observe penalty Θ^[t];
    Perform a Bernoulli trial with success probability Θ^[t]
      and record outcome Θ̃^[t];
    if Θ̃^[t] = 1 then
        α_{i*}^[t] = α_{i*}^[t] + 1;
    else
        β_{i*}^[t] = β_{i*}^[t] + 1;
    end
end
```

In (17), we set a timeout for learning at each iteration. Specifically, if a beam sweeping process is not successful within a period of D_{ref}, the observed penalty will be set to be 1. This way, the system would not wait to observe a beam sweeping process with a delay larger than D_{ref}, as the corresponding beamwidth is highly unlikely to be optimal.

VII. Performance Evaluation

In this section, we first show the impact of beamwidth on beam sweeping delay via numerical results. Then, we evaluate the performance of the proposed schemes with simulations. The operating frequency is set to 28 GHz and the NYU channel model described in [12] is implemented. Between the two bandwidth options for an SS block in 5G standards, we select the numerology 3, which corresponds to a 28.8 MHz bandwidth. The values of N_{SS} and T_{SS} are set to 64 and 20 ms, respectively. The BS transmit power is set to 30 dBm, and the minimum SNR required for signal detection is set to 0 dB. Unless otherwise specified, the number of UE antennas M_{UE} is set to 4 and the BS density ρ_{BS} is set to 10 $\mathrm{BS}/\mathrm{km}^2$.

The numerical result for average beam sweeping delay versus BS beamwidth is shown Fig. 1(a). We observe that the delay first decreases as the beam sweeping overhead reduces, and then increases as the effect of misdetection becomes dominant, causing more rounds of beam sweeping. Besides, there exists a unique value for the BS beamwidth that minimizes the expected beam sweeping delay.

We then present our simulation results. To demonstrate the effectiveness of solutions in the two stages, we consider the scheme that only applies first-stage optimization (termed proposed w/o TS) and the scheme that applies optimization of both stages (termed proposed w/ TS). We compare the delay performance of the proposed schemes with the classical fixed beamwidth scheme (termed fixed) that sets N_{tot} to be equal to N_{SS}. In the simulations, we take the coherence time of a wireless channel into account and generate a new channel instance for every T_c seconds. When a new channel is generated, it may be in three different states: LOS, NLOS, and

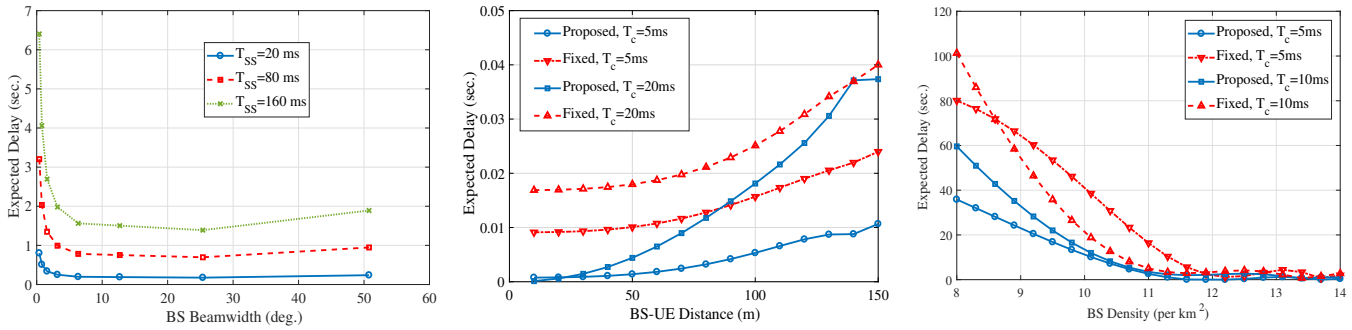

(a) (b) (c)

Fig. 1. Simulation results. (a) average delay versus BS beamwidth, (b) average delay versus BS-UE distance, (c) average delay versus BS density ρ_{BS}.

outage, following the probabilities given in [12]. The delay performance of different schemes is presented in Fig. 1(b). We can see that the proposed schemes outperform the fixed beamwidth scheme with a significantly lower delay, showing the effectiveness of beamwidth optimization in the first stage. With TS-based beamwidth adaptation, the delay can be further lowered by more than 15% on average. In particular, the performance gain is relatively larger when the distance is small, since the proposed schemes select the wider beams when the channel condition is good, while the fixed beamwidth scheme sticks to the setting $N_{\rm BS}^{(1)}N_{\rm UE}^{(1)} + N_{\rm BS}^{(2)}N_{\rm UE}^{(2)} = N_{\rm SS}$.

Figs. 1(c) presents the average delay versus BS densities. The proposed schemes achieve much lower average delay especially when $\rho_{\rm BS}$ is at a moderate range, since the BSs can optimize their beamwidths based on $\rho_{\rm BS}$. In addition, the TS algorithm enables each BS to learn the optimal beamwidth from the environment and further reduce the delay.

VIII. Conclusions

In this paper, we investigated the problem of beamwidth optimization in 5G NR mmWave cellular networks, with the objective of minimizing the beam sweeping delay during IA. We first formulated the beamwidth optimization problem. Then, we proposed solution algorithms to obtain the optimal beamwidths at BS and UE. Simulation results showed that the proposed schemes achieve more than 50% lower delay on average compared to the classical fixed beamwidth scheme.

Acknowledgment

This research was supported in part by NSF (grants CNS-1910348, CNS-1563655, CNS-1731164, CNS-1813401, and IIP-1822071) and by the Broadband Wireless Access & Applications Center (BWAC). Any opinions, findings, conclusions, or recommendations expressed in this paper are those of the author(s) and do not necessarily reflect the views of NSF.

References

[1] J. G. Andrews, *et al.,* "What will 5G be?" *IEEE J. Sel. Areas Commun.,* vol. 32, no. 6, pp. 1065–1082, June 2014.

[2] J. Wang *et al.,* "Beam codebook based beamforming protocol for multi-Gbps millimeter-wave WLAN systems," *IEEE J. Sel. Areas Commun.,* vol. 27, no. 8, pp. 1390–1399, Oct. 2009.

[3] Z. Xiao, P. Xia, and X.-G. Xia, "Codebook design for millimeter-wave channel estimation with hybrid precoding structure," *IEEE Trans. Wireless Commun.,* vol. 16, no. 1, Jan. 2017

[4] H. Shokri-Ghadikolaei, C. Fischione, G. Fodor, P. Popovski, and M. Zorzi, "Millimeter wave cellular networks: A MAC layer perspective," *IEEE Trans. Commun.,* vol. 63, no. 10, pp. 3437–3458, Oct. 2015.

[5] Y. Li, J. G. Andrews, F. Baccelli, T. D. Novlan, and C. J. Zhang, "Design and analysis of initial access in millimeter wave cellular networks," *IEEE Trans. Wireless Commun.,* vol. 16, no. 10, pp. 6409–6425, Oct. 2017.

[6] J. G. Andrews, F. Baccelli, and R. K. Ganti, "A tractable approach to coverage and rate in cellular networks," *IEEE Trans. Commun.,* vol. 59, no. 11, pp. 3122–3134, Nov. 2011.

[7] M. Giordani, M. Polese, A. Roy, D. Castor, and M. Zorzi, "A tutorial on beam management for 3GPP NR at mmWave frequencies," *IEEE Commun. Survey and Tutorials,* DOI: 10.1109/COMST.2018.2869411.

[8] 3GPP, "NR - Physical channels and modulation - Release 15," TS 38.211, V15.0.0, 2018.

[9] Ericsson, "5G New Radio: Designing for the future," Ericsson Technology Review, 2017.

[10] 3GPP, "NR PRACH preamble resource allocation," Ericsson - Tdoc R1-1611905, 2016.

[11] R. S. Elliot, Antenna theory and design. John Wiley & Sons, 2006.

[12] M. R. Akdeniz, Y. Liu, M. K. Samimi, S. Sun, S. Rangan, T. S. Rappaport, and E. Erkip, "Millimeter wave channel modeling and cellular capacity evaluation," *IEEE J. Sel. Areas Commun.,* vol. 32, no. 6, pp. 1164–1179, June 2014.

[13] C. N. Barati, S. A. Hosseini, S. Rangan, P. Liu, T. Korakis, S. S. Panwar, and T. S. Rappaport, "Directional cell discovery in millimeter wave cellular networks," *IEEE Trans. Wireless Commun.,* vol. 14, no. 12, pp. 6664–6678, Dec. 2015.

[14] C. N. Barati, S. A. Hosseini, M. Mezzavilla, T. Korakis, S. S. Panwar, S. Rangan, and M. Zorzi, "Initial access in millimeter wave cellular systems," *IEEE Trans. Wireless Commun.,* vol. 15, no. 12, pp. 6664–6678, Dec. 2016.

[15] A. Alkhateeb, Y.-H. Nam, M. S Rahman, J. Zhang, and R. W. Heath, "Initial beam association in millimeter wave cellular systems: Analysis and design insights," *IEEE Trans. Wireless Commun.,* vol. 16, no. 5, pp. 2807–2821, May 2017.

[16] H. Hassanieh, O. Abari, M. Rodriguez, M. Abdelghany, D. Katabi, and P. Indyk, "Fast millimeter wave beam alignment," in *Proc. ACM SIGCOMM'18,* Budapest, Hungary, Aug. 2018, pp. 432–445.

[17] I. Aykin and M. Krunz, "FastLink: An efficient initial access protocol for millimeter wave systems," in *Proc. ACM MSWiM'18,* Montreal, Canada, Oct. 2018, pp. 109–117.

[18] Y. Yang, H. S. Ghadikolaei, C. Fischione, M. Petrova, and K. W. Sung, "Reducing initial cell-search latency in mmwave networks," *IEEE INFOCOM'18 WKSHPS,* Honolulu, HI, Apr. 2018, pp. 686–691.

[19] I. Aykin, B. Akgun, and M. Krunz, "Smartlink: Exploiting channel clustering effects for reliable millimeter wave communications," in *Proc. IEEE INFOCOM'19,* Paris, France, Apr. 2019, pp. 1117–1125.

[20] T. Bai and R. W. Heath, "Coverage and rate analysis for millimeter-wave cellular networks," *IEEE Trans. Wireless Commun.*, vol. 14, no. 2, pp. 1100–1114, Feb. 2015.

[21] I. Aykin, B. Akgun, M. Feng, and M. Krunz, "MAMBA: A multi-armed bandit framework for beam tracking in millimeter-wave systems," in *Proc. IEEE INFOCOM'20,* Online, July 2020, pp. 1469–1478.

[22] S. Agrawal and N. Goyal, "Analysis of Thompson sampling for the multi-armed bandit problem," in *Proc. of the 25th Annual Conference On Learning (COLT)*, vol. 23, pp. 39.1–39.26, June 2012.